

Synthesis of a Fe₃O₄-CuO@meso-SiO₂ nanostructure as a magnetically recyclable and efficient catalyst for styrene epoxidation†

Cite this: DOI: 10.1039/c4cy00430b

Xiaowei Zhang,^a Ge Wang,^{*a} Mu Yang,^a Yi Luan,^a Wenjun Dong,^{*b} Rui Dang,^{ab} Hongyi Gao^a and Jie Yu^a

A novel hybrid Fe₃O₄-CuO@meso-SiO₂ catalyst was successfully fabricated by a multi-step assembly method. CuO nanoparticles were first deposited on the surface of Fe₃O₄ microspheres to form the Fe₃O₄-CuO hybrid microspheres through a solvothermal reaction. A mesoporous silica (meso-SiO₂) shell, with perpendicularly aligned pore channels, was then coated on the hybrid microspheres using sol-gel technology. The Fe₃O₄ microspheres not only offered fast and effective recycling properties for the catalyst but also acted as electron donors to CuO, leading to a higher electron density on the CuO surface and a subsequently enhanced catalytic performance. The mesoporous silica shell provided strong protection against the aggregation and leaking of the active CuO nanoparticles and also offered appropriate channels for an efficient mass transfer of the catalytic reaction. The Fe₃O₄-CuO@meso-SiO₂ catalyst exhibited excellent activity, convenient magnetic separability and good stability in the catalytic epoxidation of styrene.

Received 6th April 2014,
Accepted 8th May 2014

DOI: 10.1039/c4cy00430b

www.rsc.org/catalysis

1. Introduction

Olefin epoxides play an important role in the production of fine chemicals and pharmaceuticals.¹⁻⁶ In particular, styrene epoxide, as a promising chemical intermediate, has attracted enormous attention for the synthesis of complex organic compounds and commodity chemicals.⁷⁻⁹ It is well known that catalysts play a key role in the epoxidation of styrene, and different catalysts commonly lead to diverse oxidation products.¹⁰ Thus, the development of suitable catalysts with high catalytic activity and selectivity has become an increasingly important issue in the production of styrene epoxide.

Up until now, various types of catalysts have been developed for styrene epoxidation, such as titanium-based mesoporous catalysts¹¹⁻¹³ and noble metal catalysts.^{14,15} However, titanium-based mesoporous catalysts have shown either poor activity or low selectivity for epoxides, whereas noble metal catalysts exhibit an improved catalytic performance but at the

expense of high costs and harsh synthesis conditions. Recently, research has focused on hybrid catalysts consisting of low-cost and functional transition metal oxides.¹⁶⁻¹⁸ Hybrid nanocatalysts usually exhibit unique compositions, shape-dependent characteristics,¹⁹⁻²¹ and superior properties.²²⁻²⁵ For example, Ye *et al.*²⁶ prepared a CuO@Ag hybrid catalyst by depositing CuO nanoparticles on uniform Ag nanowires, and it showed a higher selectivity for styrene epoxide than that for CuO itself.²⁷ However, few studies have been conducted on nanohybrid catalysts consisting entirely of non-noble metals or metal oxides. It is well known that nanocatalysts tend to aggregate and have difficulties in separating and recovering from the liquid catalytic reaction system, which remains a typical problem.^{28,29}

Magnetic nanoparticles are a kind of environmentally benign support material for the immobilization of active nanocatalysts, and their magnetic response provides an efficient separation and recovery strategy for composite catalysts.³⁰⁻³⁴ Further, a mesoporous shell can protect the nanoparticles from aggregation and at the same time allow the transportation of the reactants and products,³⁵⁻³⁷ such as the multifunctional Fe₃O₄@SiO₂-Au@mSiO₂ catalyst.³⁷ Unfortunately, developing an efficient hetero-nanohybrid catalyst without a noble component *via* easy and efficient methods is rather challenging. CuO, a low-cost, naturally abundant and environmentally friendly transition metal oxide, exhibits good catalytic performance.³⁸ Many studies

^a School of Materials Science and Engineering, University of Science and Technology Beijing, Beijing 100083, China. E-mail: gewang@mater.ustb.edu.cn; Fax: +86 10 62327878; Tel: +86 10 62333765

^b Center for Nanoscience and Nanotechnology, Department of Physics, Zhejiang Sci-tech University, Hangzhou 310018, China. E-mail: wenjundong@zstu.edu.cn; Fax: +86 571 86843587; Tel: +86 571 86843587

† Electronic supplementary information (ESI) available: FT-IR spectra of Fe₃O₄ (PAA) and Fe₃O₄-CuO@meso-SiO₂; SEM, XRD and the catalytic testing data of the as-synthesized CuO nanoparticles. See DOI: 10.1039/c4cy00430b

have found that CuO is also capable of catalysing olefin epoxidation reactions.^{39–41} However, the catalytic efficiency and recovery properties still need to be improved.

In this paper, a novel heteronanostructure catalyst with a Fe₃O₄–CuO nanohybrid core and a tunable mesoporous silica shell was prepared. The PAA decorated Fe₃O₄ microspheres were first synthesized *via* a one-pot solvothermal method. With the assistance of the –COOH groups of the PAA, a small amount of CuO nanoparticles were directly deposited on the surface of the Fe₃O₄ microspheres to obtain the Fe₃O₄–CuO nanohybrid, and then a mesoporous shell was coated on the hybrid microspheres. The catalytic epoxidation of styrene was tested with the Fe₃O₄–CuO@meso-SiO₂ catalyst, and the effects of the composition and structure of the as-prepared catalyst on the catalytic performance were investigated in detail. Fe₃O₄ provided magnetic-separation properties for the entire catalyst and also offered electrons for CuO nanoparticles on the surface of the Fe₃O₄–CuO, thus possibly enhancing the catalytic activity of CuO. The mesoporous SiO₂ shell with perpendicularly aligned pore channels not only offered a physical shield to prevent the aggregation and leaching of the Fe₃O₄–CuO nanoparticles but also provided mass-transfer channels for the catalytic reaction, thus enhancing the catalytic activity. The unique nanostructure and multiple functionalities make the composite a highly efficient, low-cost and long-life catalyst with magnetic separation abilities and good reusability.

2. Experimental section

2.1 Chemicals

Ethylene glycol, sodium acetate (NaAc), cupric nitrate trihydrate (Cu(NO₃)₂·3H₂O), urea ((NH₂)₂CO), cetyltrimethylammonium bromide (CTAB), ammonia solution (25 wt.%), tetraethyl orthosilicate (TEOS), acetonitrile and *t*-butylhydroperoxide (TBHP, 70% aq.) were purchased from the Beijing Chemical Reagent Company. Ferric chloride hexahydrate (FeCl₃·6H₂O), polyvinyl pyrrolidone (PVP; Mw = 58 000), nitrobenzene, styrene, norbornene, *cis*-stilbene and *cis*-cyclooctene were obtained from Alfa Aesar. Poly(acrylic acid) (PAA; Mw = 1800), *trans*- β -methylstyrene and *trans*-stilbene were purchased from Sigma-Aldrich. All chemicals were of analytical grade and used as received without further purification.

2.2 Catalyst preparation

Preparation of the Fe₃O₄–CuO microspheres. PAA decorated Fe₃O₄ microspheres were first prepared according to our previous report.⁴² The CuO nanoparticles were deposited on the surface of the Fe₃O₄ microspheres to obtain the Fe₃O₄–CuO microspheres through a solvothermal reaction. Briefly, PVP (0.60 g) was dissolved in 150 mL of absolute ethanol, and then Cu(NO₃)₂·3H₂O (0.12 g) and (NH₂)₂CO (0.06 g) were added under ultrasound to form a homogeneous solution. The as-prepared Fe₃O₄ microspheres (0.10 g) were then added into the above solution under an

ultrasound treatment. Subsequently, the obtained solution was transferred into a Teflon-lined stainless-steel autoclave (200 mL capacity) and heated at 180 °C for 1 h. The autoclave was then cooled naturally. The product of the Fe₃O₄–CuO microspheres was separated with a magnet, washed with ethanol several times, and dried under vacuum at room temperature.

As a control, pure CuO particles were prepared using the same procedure except that no Fe₃O₄ microspheres were added into the synthesis process.

Synthesis of Fe₃O₄–CuO@meso-SiO₂ microspheres. A mesoporous silica shell was coated on the surface of the Fe₃O₄–CuO microspheres according to a modified sol-gel procedure.⁴³ 0.3 g of CTAB was dissolved into a mixed solution of ethanol (60 mL), water (80 mL) and ammonia solution (1.0 mL, 25 wt.%) under ultrasound. 0.1 g of Fe₃O₄–CuO microspheres was then dispersed into the above solution, and 0.30 g of TEOS was added drop-wise with stirring. After 6 h of continuous stirring, the product was collected, washed with ethanol, and then dried in a vacuum oven at room temperature. The mesoporous SiO₂ coated Fe₃O₄–CuO (Fe₃O₄–CuO@meso-SiO₂) microspheres were finally obtained by removing CTAB with acetone (reflux at 80 °C for 48 h).

2.3 Characterization

Field-emission scanning electron microscopy (FESEM) photographs were taken using a SUPRA 55 (Zeiss, Germany) instrument operated at 10 kV. High-resolution transmission electron microscopy (HRTEM) images were obtained using a FEI Tecnai F20 electron microscope operated at an acceleration voltage of 200 kV. Fourier-transform infrared (FT-IR) spectra were obtained with a Nicolet 6700 spectrometer. Powder X-ray diffraction (XRD) patterns were measured using a Rigaku D/MAX-RB diffractometer (40 kV, 150 mA) with a Cu K α radiation ($\lambda = 1.5406 \text{ \AA}$). Small-angle X-ray diffraction (SAXRD) patterns were recorded with a D/MAX-2550 HB/PC diffractometer (Rigaku Co., Tokyo, Japan) at 40 kV and 150 mA. Copper elemental analysis was determined with a Varian 715-ES inductively coupled plasma-atomic emission spectrometer (ICP-AES). X-ray photoelectron spectroscopy (XPS) data were collected using an Escalab 220i-XL electron spectrometer from VG Scientific with a 300 W Al K α radiation. Nitrogen adsorption was performed at 77 K using an AUTOSORB-1C analyser (USA Quantachrome Instruments). Measurements of the magnetic properties of the samples were carried out at room temperature using an MPMS-XL superconducting quantum interference device (SQUID). The catalytic results were identified using gas chromatography-mass spectrometry (Agilent 7890/5975C-GC/MSD).

2.4 Catalytic activity

The catalytic reaction for styrene epoxidation was carried out in a two-necked flask (25 mL capacity) fitted with a reflux

condenser, and an N₂ balloon was used to seal and balance this system. 10 mg of the Fe₃O₄-CuO@meso-SiO₂ catalyst (8 × 10⁻³ mmol Cu, determined by ICP), 5 mL of acetonitrile, 3 mmol of styrene and 3 mmol of nitrobenzene (as the internal standard for GC-MS analysis) were added into the flask and stirred for 30 min under a nitrogen atmosphere. Following this, 5 mmol of TBHP was added slowly under vigorous stirring, and then the flask was heated to a certain temperature for a desired time (details are given in Fig. 5 and Tables 1 and 2). Samples were periodically taken from the reaction mixture and analyzed by GC-MS with an HP-5 capillary column. After each catalytic reaction, the catalyst was collected using a magnet, washed with acetonitrile and ethanol several times, and then dried under vacuum for re-use.

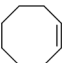


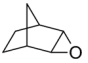
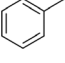
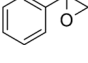
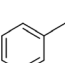
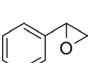
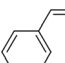
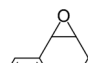
As controls, different olefins (norbornene, *trans*-β-methylstyrene, *cis*-cyclooctene, *cis*-stilbene and *trans*-stilbene) and different catalysts (CuO, Fe₃O₄-CuO, a simple mixture of Fe₃O₄ and CuO) were prepared using the same experimental procedure.

Table 1 Epoxidation of styrene with different as-synthesized products^a

Entry	Samples	Conversion (%)	Selectivity (%)
1	—	19	72
2	CuO	82	75
3	Fe ₃ O ₄ -CuO	91	86
4	Mixture of Fe ₃ O ₄ and CuO	83	74
5	Fe ₃ O ₄ -CuO@meso-SiO ₂	100	93

^a Reaction conditions: 0.27 mol% of the catalyst, 3 mmol of styrene, and 5 mmol of TBHP were stirred in 5 mL of acetonitrile at 80 °C for 7.5 h; nitrobenzene was used as the internal standard.

Table 2 Olefin epoxidation with different substrates^a

Entry	Substrates	Products	Time (h)	Conversion (%)	Selectivity (%)
1			14	100	>99
2			5	92	>99
3			2	100	>99
4			6	100	>99
5			24	79	>99

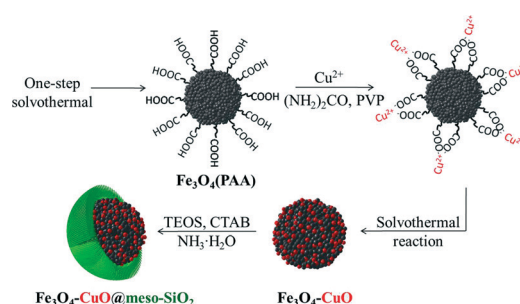
^a Reaction conditions: 0.27 mol% of the Fe₃O₄-CuO@meso-SiO₂ catalyst, 3 mmol of the substrate, and 5 mmol of TBHP were stirred in 5 mL of acetonitrile at 80 °C; nitrobenzene was used as the internal standard.

3. Results and discussion

3.1 Morphology and structure of the Fe₃O₄-CuO@meso-SiO₂ catalyst

The synthesis route of the Fe₃O₄-CuO@meso-SiO₂ microspheres is shown in Scheme 1. Initially, the PAA decorated Fe₃O₄ magnetic microspheres were synthesized by a one-step solvothermal method. The CuO nanoparticles were then deposited on the surface of the Fe₃O₄ microspheres with the assistance of PVP. Finally, a silica shell with radial mesopores was formed on the surface of the Fe₃O₄-CuO microspheres by using a template-assisted sol-gel procedure.

The Fe₃O₄-CuO nano-hybrid core is the essential part of the catalyst. In order to ensure its high magnetic responsiveness, the Fe₃O₄ core and CuO nanoparticles were synthesized. Since there were few binding groups on the naked Fe₃O₄ nanoparticles, surface modification was very necessary to provide functional linkage⁴³ for the efficient preparation of the Fe₃O₄-CuO hybrid nanocomposite. Here, the modification of PAA on the Fe₃O₄ core was able to provide functional carboxylate groups (-COOH), which favoured the subsequent coating or depositing of metal ions.⁴⁴ Cu(NO₃)₂·3H₂O and (NH₂)₂CO were then used as the starting materials and PVP as the surfactant



Scheme 1 The synthesis process of the Fe₃O₄-CuO@meso-SiO₂ material.

to complete the partial deposition of CuO. Herein, the Cu^{2+} in the $\text{Cu}(\text{NO}_3)_2 \cdot 3\text{H}_2\text{O}$ precursor could be anchored on the surface of $\text{Fe}_3\text{O}_4(\text{PAA})$ by the $-\text{COOH}$ groups. Furthermore, hydroxyl groups generated from the hydrolysis of urea³⁹ along with a powerful morphology-controlling surfactant (PVP)⁴⁵ could promote the formation of the spherical CuO nanoparticles.⁴⁶ In order to enhance the interaction between the Fe_3O_4 and CuO nanoparticles, the loading amounts of CuO had to be controlled by adjusting the addition of $\text{Cu}(\text{NO}_3)_2 \cdot 3\text{H}_2\text{O}$. Lower CuO deposition helped to expose some of the Fe_3O_4 surface, which was favourable for the formation of $\text{Fe}_3\text{O}_4\text{-CuO}$ nano-hybrids. However, excessive CuO loading would result in a compact CuO shell outside of the Fe_3O_4 core, and the isolated layers would inhibit the interaction between them. Finally, the outer mesoporous silica shell was prepared by using TEOS as the precursor and CTAB as the surfactant, and it provided a strong protective layer to avoid the loss of active metal oxides under rigorous reaction conditions.⁴³ More importantly, the open mesopore channels in the outer shell allowed for the access of guest molecules, which might have enhanced the catalytic reaction.^{43,46} The successful modification of PAA and complete removal of CTAB were verified by FT-IR spectra characterization (Fig. S1†).

The FESEM image in Fig. 1a shows that the initial PAA-decorated Fe_3O_4 microspheres were uniform with a mean diameter of 200 nm. These microspheres, with rough surfaces, were composed of many small Fe_3O_4 crystallites.⁴⁷ After the deposition of the CuO nanoparticles, the composite microspheres maintained spherical morphology and rough surfaces (Fig. 1b). The elemental maps (Fig. 1e–h) demonstrate that CuO nanoparticles were deposited on the surface of the Fe_3O_4 with good dispersion. To protect the active $\text{Fe}_3\text{O}_4\text{-CuO}$ microspheres, a mesoporous silica shell was coated using the sol-gel procedure with TEOS as the precursor and CTAB as the template. The $\text{Fe}_3\text{O}_4\text{-CuO@meso-SiO}_2$ microspheres showed clear core-shell structures (Fig. 1c, d), and the silica shell was uniform with 30 nm in thickness and composed of radially aligned mesopores (inset in Fig. 1c).

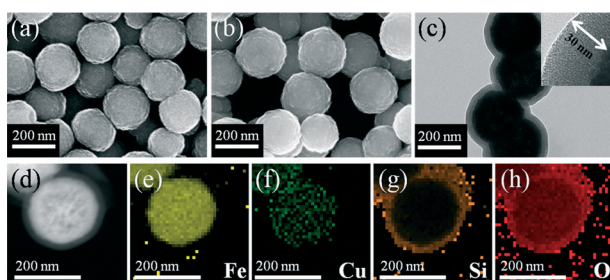


Fig. 1 FESEM images of (a) PAA decorated Fe_3O_4 microspheres, (b) $\text{Fe}_3\text{O}_4\text{-CuO}$ microsphere. (c) HRTEM images of $\text{Fe}_3\text{O}_4\text{-CuO@meso-SiO}_2$ (inset: a high-magnification HRTEM image of the silica shell). (d) High-angle annular dark field STEM (HAADF-STEM) image of a $\text{Fe}_3\text{O}_4\text{-CuO@meso-SiO}_2$ particle showing where the elemental maps were obtained and (e–h) the elemental maps of the same particle for Fe, Cu, Si and O, respectively.

The corresponding particle size distribution details are shown in Fig. S2.†

The crystalline nature and chemical composition of the as-prepared products were confirmed by powder XRD. Fig. 2 displays the XRD patterns of the Fe_3O_4 , $\text{Fe}_3\text{O}_4\text{-CuO}$ and $\text{Fe}_3\text{O}_4\text{-CuO@meso-SiO}_2$ microspheres. For the sample of the Fe_3O_4 microspheres (Fig. 2a), 2θ diffraction peaks at 30.0° , 35.3° , 42.8° , 53.3° , 56.8° and 62.6° correspond to (220), (311), (400), (422), (511), and (440) planes of cubic inverse spinel Fe_3O_4 (JCPDS 03-0863), respectively. No other characteristic peaks of impurities are observed. The crystallite size of Fe_3O_4 is 13 nm according to Scherrer's formula with the strongest peak (311). For the $\text{Fe}_3\text{O}_4\text{-CuO}$ composite microspheres (Fig. 2b), the peaks of Fe_3O_4 still exist and new diffraction peaks at 32.2° , 38.6° , 48.6° , 58.1° , 61.4° , 66.2° and 68.0° correspond to the (110), (111), (-202), (202), (-113), (-311) and (220) planes of the CuO pattern (JCPDS 05-0661), indicating successfully deposited CuO nanoparticles. The average size of the CuO crystallites was about 9 nm calculated from the (111) peak. For the $\text{Fe}_3\text{O}_4\text{-CuO@meso-SiO}_2$ catalyst (Fig. 2c), a broad diffraction peak at 23.0° can be observed, which is attributed to the amorphous silica.³⁸ The other peaks almost remain the same as those in Fig. 2b. The content of Cu in the $\text{Fe}_3\text{O}_4\text{-CuO@meso-SiO}_2$ microspheres was 5.1 wt.% according to the ICP analysis.

Nitrogen adsorption and a small-angle XRD (SAXRD) pattern were used to obtain further structural details of the $\text{Fe}_3\text{O}_4\text{-CuO@meso-SiO}_2$ microspheres. Nitrogen adsorption-desorption isotherms show type-IV curves (Fig. 3a), and the pore size distribution (inset in Fig. 3a) indicates a narrow size distribution centered at 2.4 nm. The BET surface area and total pore volume calculated by the Barrett-Joyner-Halenda (BJH) model were $465.3 \text{ m}^2 \text{ g}^{-1}$ and $0.32 \text{ cm}^3 \text{ g}^{-1}$, respectively. SAXRD shows a peak at 2.52° (Fig. 3b). These results suggest that the silica shell exhibited a relatively ordered mesoporous structure, which is well in agreement with the HRTEM results.

The magnetic properties of the as-synthesized samples were measured with a vibrating magnetometer at room temperature (Fig. 4). No hysteresis loops in the three samples indicate that they are superparamagnetic, which is in

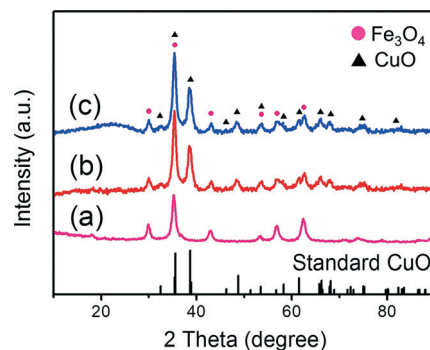


Fig. 2 Powder XRD patterns of (a) Fe_3O_4 , (b) $\text{Fe}_3\text{O}_4\text{-CuO}$, (c) $\text{Fe}_3\text{O}_4\text{-CuO@meso-SiO}_2$ microspheres and the standard CuO XRD pattern.

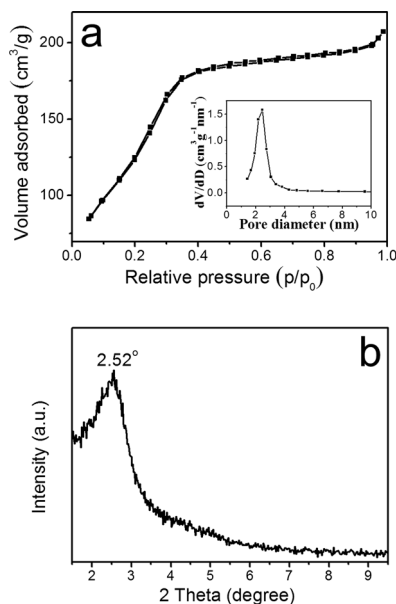


Fig. 3 (a) N_2 adsorption-desorption isotherms (inset: pore size distribution) and (b) small-angle XRD pattern of Fe_3O_4 -CuO@meso- SiO_2 microspheres.

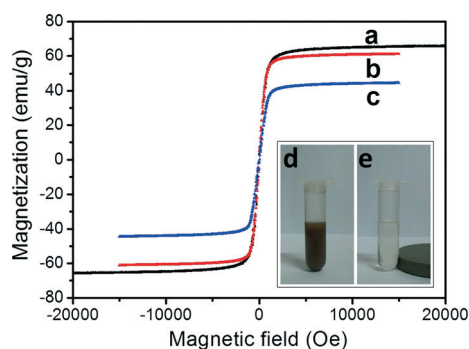


Fig. 4 Magnetic hysteresis loops of (a) Fe_3O_4 , (b) Fe_3O_4 -CuO and (c) Fe_3O_4 -CuO@meso- SiO_2 microspheres. Photographs of the Fe_3O_4 -CuO@meso- SiO_2 catalyst dispersed in ethanol (d) without magnetic field and (e) with magnetic field.

accordance with the small crystallite size of Fe_3O_4 (13 nm). The magnetization saturation values of the Fe_3O_4 (Fig. 4a), Fe_3O_4 -CuO (Fig. 4b) and Fe_3O_4 -CuO@meso- SiO_2 (Fig. 4c) microspheres are 66.2, 61.1 and 44.5 $emu\ g^{-1}$, respectively. The reduced saturation magnetization in the Fe_3O_4 -CuO and Fe_3O_4 -CuO@meso- SiO_2 samples was caused by the presence of the nonmagnetic copper and silica.⁴⁸ According to the saturation magnetization, the Fe_3O_4 -CuO@meso- SiO_2 microspheres were composed of 67 wt.% magnetite, 6 wt.% CuO and 27 wt.% SiO_2 . These results were in basic accordance with those of the ICP analysis (5.1 wt.% Cu, 6.4 wt.% CuO). With such high magnetization, Fe_3O_4 -CuO@meso- SiO_2 microspheres could be easily separated from the solution under an external magnetic field (Fig. 4d, e), which was favourable for the magnetic separation of the catalyst.

3.2 Catalytic properties

Fe_3O_4 -CuO@meso- SiO_2 microspheres were used to catalyze the epoxidation of styrene. The reaction was carried out by using 10 mg of the as-prepared catalyst (8×10^{-3} mmol Cu, determined by ICP) along with TBHP as the oxidant and acetonitrile as the solvent. The catalytic activity *versus* reaction temperature and reaction time was investigated (Fig. 5). When the temperature increased from 50 °C to 80 °C, an increase in the conversion of styrene and selectivity for styrene epoxide was observed (Fig. 5a).

At higher temperatures (90 °C and 100 °C), the conversion of styrene further increased, while the selectivity for styrene oxide decreased. When the temperature was set at 80 °C, both the conversion and the selectivity increased as the reaction time was prolonged (Fig. 5b). After 7.5 h, the substrate styrene was consumed completely (100%) with a high selectivity of 93%, which was the optimal catalytic result over the Fe_3O_4 -CuO@meso- SiO_2 composite catalyst. The turnover frequency (TOF) (TOF = mol of styrene epoxide formed per mol of Cu per second) of the Fe_3O_4 -CuO@meso- SiO_2 catalyst was $12.9 \times 10^{-3}\ s^{-1}$, which is significantly better than those catalysts reported previously.^{34,37,46}

The reusability of the Fe_3O_4 -CuO@meso- SiO_2 catalyst in the epoxidation of styrene is summarized in Fig. 6. Recycling results show that the Fe_3O_4 -CuO@meso- SiO_2 catalyst maintained a high conversion rate (100%) and selectivity (92%) after being recycled fifteen times, indicating good stability of the catalyst in the catalytic system.

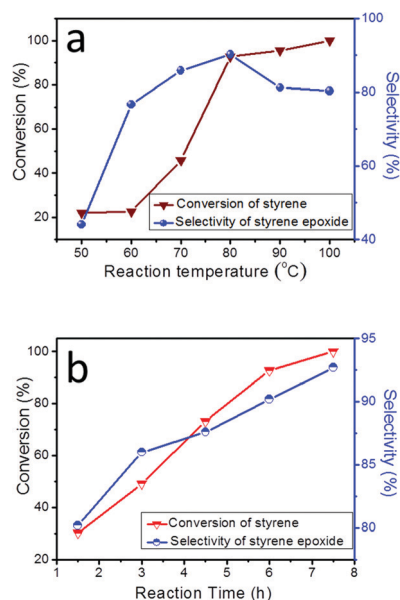


Fig. 5 The conversion of styrene and the selectivity for styrene epoxide as functions of (a) reaction temperature and (b) reaction time using an Fe_3O_4 -CuO@meso- SiO_2 catalyst. Reaction conditions: 3 mmol of styrene, 5 mmol of TBHP, and 0.27 mol% of the catalyst were stirred in 5 mL of acetonitrile for (a) a reaction time of 6 h and (b) a reaction temperature of 80 °C using nitrobenzene as the internal standard.

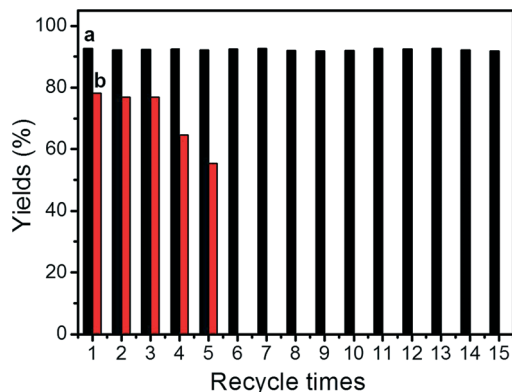


Fig. 6 Recycling results for styrene epoxidation for the catalysts of (a) Fe₃O₄-CuO@meso-SiO₂ and (b) Fe₃O₄-CuO. Reaction conditions: 3 mmol of styrene, 5 mmol of TBHP, and 0.27 mol% of the catalyst were stirred in 5 mL of acetonitrile at 80 °C for 7.5 h using nitrobenzene as the internal standard.

To investigate the effects of the components and structures of the catalyst, two sets of control experiments were also carried out.

Firstly, the catalytic activities of pure CuO, Fe₃O₄-CuO and a simple mixture of Fe₃O₄ and CuO for styrene epoxidation were studied at 80 °C (Table 1).

The pure CuO was synthesized according to the same procedure for the Fe₃O₄-CuO microspheres except that no Fe₃O₄ microspheres were added into the synthesis process. The as-prepared CuO particles were spherical with an average diameter range from 150 nm to 450 nm (Fig. S3[†]). The XRD pattern (Fig. S4[†]) showed that the CuO particles were in their tenorite phase (JCPDS no 05-0661). The conversion of styrene, the selectivity for styrene epoxide and its reaction time over the CuO particles were also tested (Fig. S5[†]). Compared to blank testing in the absence of a catalyst (Table 1, entry 1), the CuO particles showed good catalytic activity (82% conversion of styrene, 75% selectivity of styrene epoxide) after 7.5 h and the results are listed in Table 1 (entry 2). Fe₃O₄-CuO hybrids exhibited a significantly higher conversion of styrene (91%) and better selectivity for styrene epoxide (86%) (Table 1, entry 3), which may be due to the assistance of the Fe₃O₄ nanoparticles. In contrast, a simple mixture of Fe₃O₄ and CuO was also used to catalyze the same reaction (Table 1, entry 4). Results showed that the catalytic performance of the simple mixture of Fe₃O₄ and CuO was similar to that of pure CuO particles. These results indicate that only the Fe₃O₄ in the Fe₃O₄-CuO hybrids could enhance the catalytic activity of CuO nanoparticles.

The as-prepared CuO and Fe₃O₄-CuO nanoparticles were investigated by XPS (Fig. 7). As shown in Fig. 7a, the XPS detected the Cu 2p_{3/2} peak at ~934.2 eV with two shakeup satellite peaks at ~943.4 eV and ~941.9 eV, indicating the formation of CuO with a Cu²⁺ state for Cu atoms.^{49,50} Compared with the as-prepared CuO sample (Fig. 7a, 934.2 eV), the peak of Cu 2p_{3/2} in Fe₃O₄-CuO (Fig. 7b) shifted to a lower binding energy (933.4 eV), indicating that the Fe₃O₄ acted as an

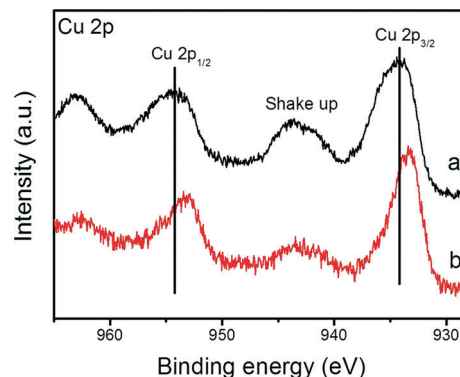


Fig. 7 XPS patterns of the as-synthesized (a) CuO and (b) Fe₃O₄-CuO nanoparticles.

electron donor to activate CuO,^{51,52} resulting in a higher electronic density on the CuO surface, thus promoting the catalytic performance of the entire catalyst.^{34,53}

Secondly, the effect of the mesoporous silica shell on catalytic properties was also studied. Compared to the Fe₃O₄-CuO nanohybrids, the Fe₃O₄-CuO@meso-SiO₂ composite exhibited better catalytic activities (Table 1, entry 5, 100% conversion, 93% selectivity). The reusability of the as-prepared Fe₃O₄-CuO was investigated as well (Fig. 6b). The yield of styrene epoxide significantly decreased after only five cycles, while the Fe₃O₄-CuO@meso-SiO₂ composite could be recycled over fifteen times, without compromising the yield and selectivity (Fig. 6a), and their structures and morphologies were almost completely maintained (Fig. S6[†]). These results indicate that the Fe₃O₄-CuO@meso-SiO₂ composite was more stable than the Fe₃O₄-CuO nanohybrids.

Compared with Fe₃O₄-CuO, the higher catalytic performance and reusability of the Fe₃O₄-CuO@meso-SiO₂ composite was attributed to the structure of the outer layer. With the large surface area and highly open and ordered mesopore channels of the silica shell, the Fe₃O₄-CuO@meso-SiO₂ catalyst could adsorb reagents, thus enriching the guest molecules around the catalyst, accelerating the mass transfer and promoting the reactions, serving as nanoreactors.^{31,36,54} Meanwhile, the silica shell with a small pore size (2.4 nm) could prevent CuO crystallites (9 nm) and Fe₃O₄ (13 nm) from leaching, which enhanced the stability of the as-prepared Fe₃O₄-CuO@meso-SiO₂ catalyst.

To determine the general applicability of the Fe₃O₄-CuO@meso-SiO₂ catalyst, epoxidation reactions of *cis*-cyclooctene, norbornene, *trans*-β-methylstyrene, *trans*-stilbene and *cis*-stilbene were also studied, and the results are summarized in Table 2. The *cis*-cyclooctene can be quantitatively converted to epoxyoctane with high selectivity (>99%) after 14 h (Table 2, entry 1). Our optimal reaction conditions were also suitable for the epoxidation of norbornene, which provides the desired epoxide in 92% yield (Table 2, entry 2). β-Substituted styrene, such as *trans*-β-methylstyrene, gave a 100% conversion and >99% selectivity to its corresponding epoxide product after 2 h. Methyl substitution inhibited the

formation of the benzaldehyde by-product generated through the oxidative cleavage pathway, which offers much improved results in terms of selectivity and yield (Table 2, entry 3). For the epoxidation of stilbene, *trans*-stilbene transformed to its corresponding epoxide much faster than *cis*-stilbene due to the steric effect (Table 2, entries 4 and 5). The high conversion and selectivity of the corresponding epoxides indicate that the catalytic activity enhancement was from the composition of Fe₃O₄ nanoparticles and the uniform silica shell in the Fe₃O₄-CuO@meso-SiO₂ composite, and the synergistic effects among the three components (Fe₃O₄, CuO and meso-SiO₂) made the as-prepared Fe₃O₄-CuO@meso-SiO₂ composite an efficient and stable catalyst for the olefin epoxidation reactions. As a result, our catalytic system performed much more efficiently than any other system reported in the literature employing *t*-BuOOH as the oxidant.^{34,37,46}

4. Conclusions

A novel magnetically recyclable and highly efficient core-shell Fe₃O₄-CuO@meso-SiO₂ catalyst was designed and synthesized for styrene epoxidation. The components and the structure of the composite microspheres provided the hybrid catalyst with improved catalytic properties and attractive features. Fe₃O₄ microspheres could be used not only as a functional support with good dispersion and magnetic separation but also as a co-catalyst *via* offering electrons to CuO, and subsequently promoting its catalytic activity. The mesoporous SiO₂ shell with perpendicularly aligned pore channels offered a physical shield to prevent the aggregation and outflow of the CuO and Fe₃O₄ nanoparticles, and it provided mass transfer channels for the catalytic reaction as well. Therefore the multifunctional catalyst with well-designed structures provides a highly efficient, well-dispersed, easily separated, and excellently circulated catalytic system for styrene epoxidation. This strategy may be extended to the design of multifunctional nanohybrids that contain catalytically active metals/metal oxides other than CuO.

Acknowledgements

We would like to thank the PetroChina Innovation Foundation (no. 2012D-5006-0504) and the National High Technology Research and the Development Program of China (863 Program) (no. 2013AA031702) for their support.

Notes and references

- Q. H. Xia, H. Q. Ge, C. P. Ye, Z. M. Liu and K. X. Su, *Chem. Rev.*, 2005, **105**, 1603.
- J. Hu, *J. Phys. Chem. C*, 2013, **117**, 16005.
- W. Zhang, J. L. Loebach, S. R. Wilson and E. N. Jacobsen, *J. Am. Chem. Soc.*, 1990, **112**, 2801.
- K. Yamaguchi, K. Ebitani and K. Kaneda, *J. Org. Chem.*, 1999, **64**, 2966.
- R. R. Sever and T. W. Root, *J. Phys. Chem. B*, 2003, **107**, 4090.
- R. A. Sheldon, M. Wallau and I. W. C. E. Arends, *Acc. Chem. Res.*, 1998, **31**, 485.
- B. Singh and A. K. Sinha, *J. Mater. Chem. A*, 2014, **2**, 1930.
- K. Parida, K. G. Mishra and S. K. Dash, *Ind. Eng. Chem. Res.*, 2012, **51**, 2235.
- W. C. Zhan, Y. L. Guo, Y. Q. Wang, Y. Guo, X. H. Liu, Y. S. Wang, Z. G. Zhang and G. Z. Lu, *J. Phys. Chem. C*, 2009, **113**, 7181.
- V. Hulea and E. Dumitriu, *Appl. Catal., A*, 2004, **277**, 99.
- A. M. Balua, J. M. Hidalgo, J. M. Campelob, D. Luna, R. Luquea, J. M. Marinas and A. A. Romerob, *J. Mol. Catal. A: Chem.*, 2008, **293**, 17.
- M. G. Clerici and P. Ingallina, *J. Catal.*, 1993, **140**, 71.
- C. A. Müller, M. Maciejewski, T. Mallat and A. Baiker, *J. Catal.*, 1999, **184**, 280.
- Y. M. Liu, H. Tsunoyama, T. Akita and T. Tsukuda, *Chem. Commun.*, 2010, **46**, 550.
- Y. Jin, D. Y. Zhuang, N. Y. Yu, H. H. Zhao, Y. Ding, L. S. Qin, J. F. Liu, D. H. Yin, H. Y. Qiu, Z. H. Fu and D. L. Yin, *Microporous Mesoporous Mater.*, 2009, **126**, 159.
- K. Drew, G. Girishkumar, K. Vinodgopal and V. K. Prashant, *J. Phys. Chem. B*, 2005, **109**, 11851.
- Z. M. Yang, G. F. Huang, W. Q. Huang, J. M. Wei, X. G. Yan, Y. Y. Liu, C. Jiao, Z. Wan and A. L. Pan, *J. Mater. Chem. A*, 2014, **2**, 1750.
- H. Wang, J. Shen, Y. Y. Li, Z. Y. Wei, G. X. Cao, Z. Gai, K. L. Hong, P. Banerjee and S. Q. Zhou, *ACS Appl. Mater. Interfaces*, 2013, **5**, 9446.
- E. Gianotti, U. Diaz, A. Velty, T. Tsuda and A. Corma, *Catal. Sci. Technol.*, 2013, **3**, 2677.
- D. H. Sun, G. L. Zhang, X. D. Jiang, J. L. Huang, X. L. Jing, Y. M. Zheng, J. He and Q. B. Li, *J. Mater. Chem. A*, 2014, **2**, 1767.
- P. Li, Z. Wei, T. Wu, Q. Peng and Y. D. Li, *J. Am. Chem. Soc.*, 2011, **133**, 5660.
- H. Y. Yan, Z. Y. Bai, S. J. Chao, L. Yang, Q. Cui, K. Wang and L. Niu, *RSC Adv.*, 2013, **3**, 20332.
- C. H. A. Tsang, Y. Liu, Z. H. Kang, D. D. D. Ma, N. B. Wong and S. T. Lee, *Chem. Commun.*, 2009, 5829.
- N. Zhang, S. Q. Liu, X. Z. Fu and Y. J. Xu, *J. Phys. Chem. C*, 2011, **115**, 22901.
- L. Y. Jin, R. H. Ma, J. J. Lin, L. Meng, Y. J. Wang and M. F. Luo, *Ind. Eng. Chem. Res.*, 2011, **50**, 10878.
- Z. M. Ye, L. Hu, J. Jiang, J. X. Tang, X. Q. Cao and H. W. Gu, *Catal. Sci. Technol.*, 2012, **2**, 1146.
- G. H. Qiu, S. Dharmarathna, Y. S. Zhang, N. Opembe, H. Huang and S. L. Suib, *J. Phys. Chem. C*, 2012, **116**, 468.
- Y. Yang, J. Liu, X. B. Li, X. Liu and Q. H. Yang, *Chem. Mater.*, 2011, **23**, 3676.
- J. C. Park, J. U. Bang, J. Lee, C. H. Ko and H. Song, *J. Mater. Chem.*, 2010, **20**, 1239.
- A. Pourjavadi, S. H. Hosseini, M. Doulabi, S. M. Fakoorpoor and F. Seidi, *ACS Catal.*, 2012, **2**, 1259.
- J. P. Ge, T. Huynh, Y. X. Hu and Y. D. Yin, *Nano Lett.*, 2008, **8**, 931.

- 32 A. Q. Wang, X. Liu, Z. X. Su and H. W. Jing, *Catal. Sci. Technol.*, 2014, 4, 71.
- 33 T. Zeng, X. L. Zhang, S. H. Wang, Y. R. Ma, H. Y. Niu and Y. Q. Cai, *J. Mater. Chem. A*, 2013, 1, 11641.
- 34 D. H. Zhang, G. D. Li, J. X. Li and J. S. Chen, *Chem. Commun.*, 2008, 3414.
- 35 Q. Zhang, J. P. Ge, J. Goebel, Y. X. Hu, Z. D. Lu and Y. D. Yin, *Nano Res.*, 2009, 2, 583.
- 36 Z. Chen, Z. M. Cui, P. Li, C. Y. Cao, Y. L. Hong, Z. Y. Wu and W. G. Song, *J. Phys. Chem. C*, 2012, 116, 14986.
- 37 Y. H. Deng, Y. Cai, Z. K. Sun, J. Liu, C. Liu, J. Wei, W. Li, C. Liu, Y. Wang and D. Y. Zhao, *J. Am. Chem. Soc.*, 2010, 132, 8466.
- 38 X. W. Zhang, N. Huang, G. Wang, W. J. Dong, M. Yang, Y. Luan and Z. Shi, *Microporous Mesoporous Mater.*, 2013, 177, 47.
- 39 L. P. Xu, S. Sithambaram, Y. S. Zhang, C. H. Chen, L. Jin, R. Joesten and S. L. Suib, *Chem. Mater.*, 2009, 21, 1253.
- 40 W. Qin, X. Li and J. Y. Qi, *Langmuir*, 2009, 25, 8001.
- 41 N. S. Patil, B. S. Uphade, D. G. McCulloh, S. K. Bhargava and V. R. Choudhary, *Catal. Commun.*, 2004, 5, 681.
- 42 W. C. Guo, Q. Wang, G. Wang, M. Yang, W. J. Dong and J. Yu, *Chem. – Asian J.*, 2013, 8, 1160.
- 43 Y. H. Deng, D. W. Qi, C. H. Deng, X. M. Zhang and D. Y. Zhao, *J. Am. Chem. Soc.*, 2008, 130, 28.
- 44 V. Polshettiwar, R. Luque, A. Fihri, H. Zhu, M. Bouhrara and J. M. Basset, *Chem. Rev.*, 2011, 111, 3036.
- 45 X. Y. Yu, R. X. Xu, C. Gao, T. Luo, Y. Jia, J. H. Liu and X. J. Huang, *ACS Appl. Mater. Interfaces*, 2012, 4, 1954.
- 46 C. Q. Chen, J. Qu, C. Y. Cao, F. Niub and W. G. Song, *J. Mater. Chem.*, 2011, 21, 5774.
- 47 J. P. Ge, Y. X. Hu, M. Biasini, W. P. Beyermann and Y. D. Yin, *Angew. Chem., Int. Ed.*, 2007, 46, 4342.
- 48 S. Santra, R. Tapeç, N. Theodoropoulou, J. Dobson, A. Hebard and W. Tan, *Langmuir*, 2001, 17, 2900.
- 49 J. Kim, W. Kim and K. J. Yong, *J. Phys. Chem. C*, 2012, 116, 15682.
- 50 S. F. Zheng, J. S. Hu, L. S. Zhong, W. G. Song, L. J. Wan and Y. G. Guo, *Chem. Mater.*, 2008, 20, 3617.
- 51 F. C. C. Moura, M. H. Araujo, R. C. C. Costa, J. D. Fabris, J. D. Ardisson, W. A. A. Macedo and R. M. Lago, *Chemosphere*, 2005, 60, 1118.
- 52 H. C. Liu, A. I. Kozlov, A. P. Kozlova, T. Shido and Y. Iwasawa, *Phys. Chem. Chem. Phys.*, 1999, 1, 2851.
- 53 J. L. Shi, *Chem. Rev.*, 2013, 113, 2139.
- 54 A. Agiral, H. S. Soo and H. Frei, *Chem. Mater.*, 2013, 25, 2264.